Recent Surface Deformation along the Carmel-Gilboa Fault System, Israel

Gilad Evn-Tzur[1], Jörg Reinking[2]

[1] Division of Mapping and Geo-Information Engineering, Technion - Israel Institute of Technology, Haifa, Israel, (eventzur@technion.ac.il)
[2] Department of Civil Engineering and Geoinformation, Jade University of Applied Sciences, Oldenburg, Germany

Key words: *Carmel-Gilboa Fault System; Velocity field; Extended free Network; GPS*

ABSTRACT

The Carmel-Gilboa Fault System is one of the major geological structures of northern Israel. It is a northwestern branch of the Dead Sea Fault. Tectonic activity and crustal deformation occur along the Carmel Gilboa Fault System. The fault system region is covered by a monitoring geodetic network consisting of 24 sites. In this paper we analyze GPS data which were measured eight times between 1999 and 2016 and derive regional velocities for the network sites. The site velocities were estimated with respect to a local datum. In order to define a correct datum and ensure stability of the datum we assume that GPS vectors are not immune to changes in their datum content of orientation and scale. The GPS vectors from each campaign are stripped from their datum content using the extended free network adjustment constraints. The datumless measurements are used to define the datum by preliminary coordinates and linear constraints, which remain constant for all monitoring campaigns, as well as to define the position of the network points and their velocities. The use of extended S-transformation enables transition from one datum to another and calculates the velocities in relation to the chosen datum.

We use principles from continuum mechanics to extract the horizontal site velocities field into surface deformation parameters. The results show deformations of about 1 mm/yr sinister along the Carmel Gilboa Fault System accompanied with extensions and shear strain.

I. INTRODUCTION

Tectonic activity and crustal deformation in northern Israel occur mainly on the Dead Sea Fault (DSF) and the Carmel-Gilboa Fault System (CGFS). The DSF is a sinistral transform fault that forms the boundary between the Arabian Plate and the Sinai Sub-Plate mainly on the N-S trending (Fig 1). The CGFS is composed of several NW-SE trending faults while the main faults are the Carmel Fault (CF) and Gilboa Fault (GF) (Fig. 2). The CGFS is a branch of the DSF that starts at the Jordan Valley, goes up to the northern tip of Mount Carmel and extends into the Mediterranean Sea.

There is no agreement on the exact location of the CGFS. There are those who locate the main fault along the southwestern side of the Yizre'el Valley (for example, Hofstetter et al., 1996; Rotstein et al., 2004; Fleischer and Gafsou, 2005) and others locate the main fault somewhere within the Yizre'el Valley downfaulted structure (Segev and Rybakov, 2011). Actually, the CGFS is a wide (up to ~20 km) deformation zone on the valley's southeastern side, which narrows towards the northwest (Mount Carmel). The fault pattern within the Yizre'el Valley is not well known. Some suggested a fault system below the Yizre'el Valley, which connects the Gilboa and the Carmel faults (Segev et al., 2006; Segev et al., 2014).

Mount Carmel is an elevated and intensively faulted area that is bordered by the main Carmel Fault on the northeast. The latter is divided into two main segments: A NW-SE oriented segment that runs from Haifa Bay towards Amaqim Junction (Jalame) and a N-S oriented fault that runs between Jalame and Yoqneam (Fig. 2). Its continuation southward is the Yoqneam Fault.

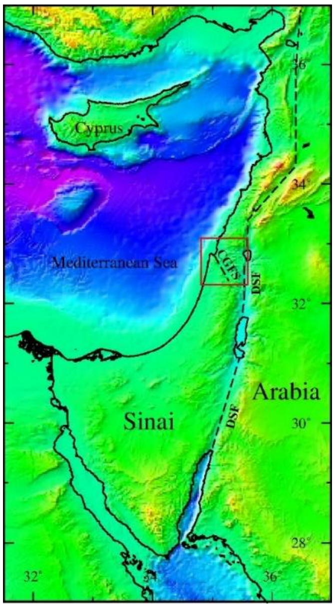

Figure 1. Tectonic map of Eastern Mediterranean showing the Sinai and Arabia plates. The black dash line denotes the location of the Dead Sea Fault (DSF). The red box denotes the study area with the Carmel Gilboa Fault System (CGFS) location.

In this study we implement the extended free network adjustment constraints solution (Even-Tzur, 2011) to calculate the velocities of 24 sites that were measured eight times between 1999 and 2016 using GPS. The outcome is a velocity field covering the Carmel Fault region. Since the accuracy of vertical position is low relative to horizontal position, we only estimated the horizontal site velocities. The local datum is taken into account by extended similarity transformation (Even-Tzur, 2012), that allows for transforming the coordinates of network sites to any desired datum.

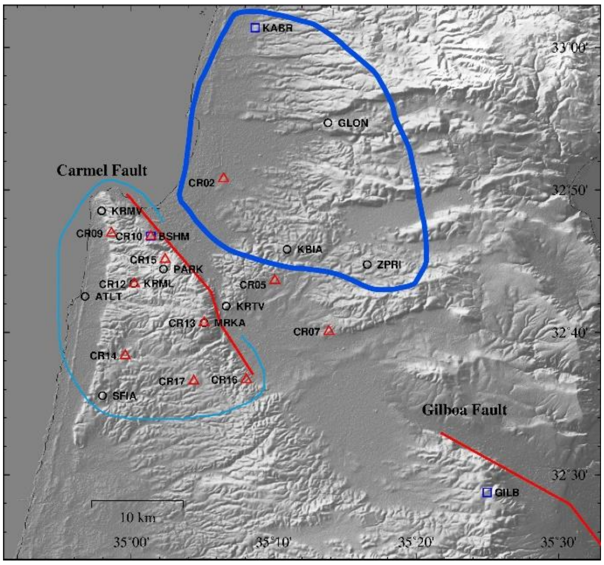

Figure 2. The digital elevation map of the study area with the location of the Carmel Gilboa Fault System and GPS sites used in this analysis. Blue squares: APN sites. Black circles: G1 sites. Red triangles: CR sites. The Blue line denote the Galilee datum points. The Azure line denote the tested points.

II. THE GPS NETWORK, CAMPAIGNS AND DATA PROCESSING

The CGFS region is covered by a geodetic monitoring network, consisting of 24 sites (Fig. 2) that were measured in 1999, 2006, 2009, 2010, 2011, 2012, 2014 and 2016 by means of GPS. The network that was used to determine the velocity field consists of three parts that are combined in observation and analysis: The Carmel network, the G1 network and three sites of the Israeli network of permanent GNSS sites (APN, Active Permanent Network). The Carmel network (CR) was established in 1990 to monitor horizontal movements in the Carmel region. Today the network is composed of 11 points (Fig. 2, red triangles). The network points were marked, without any exception, on exposed and solid bedrock. The G1 network was designed and established in the beginning of the 1990s with the intention of monitoring crustal deformation and serving as the major control network in Israel. The marks were built according to high technical specifications to ensure their geotechnical stability. Ten G1 sites were measured (Fig. 2, black circles), two of them are located close to two sites of CR, enabling a double check of the resulting site velocities. Additionally, data from four sites (ELAT, RAMO, TELA KATZ, BSHM, KABR and GILB) of the Israeli network of permanent GPS sites (APN) and three supplementary IGS sites (NICO, ANKR and ZECK) are included in the GPS analysis. Three of the APN sites (Fig. 2, blue squares) are in the vicinity of the network and therefore are incorporated in the deformation analysis. One of the sites (BSHM) is close to another CR network site.

The non-permanent sites were occupied using tripods for the CR network sites while the G1 network sites were measured using special centering devices, which allow an easier setup of the antenna. All sites were occupied at least twice in each campaign with observation time spans of 4 h for the 1999 campaign and 8 h for all the other campaigns (2006 until 2016). In all campaigns dual-frequency receivers were used. In 1999 and 2006 campaigns choke ring antennas were used along with geodetic antennas, since 2009 choke ring antennas were used exclusively.

In total, GPS data from 31 sites were incorporated into the analysis process. The GPS data analysis was done using the Bernese GNSS Software Version 5.2 (Dach et al., 2015). All campaigns were processed using precise ephemeris, EOPs and absolute antenna phase center variations with respect to IGS08 (http://igscb.jpl.nasa.gov). To ensure the consistency of all campaign solutions we introduced the IGS coordinates from the weekly solution for IGS stations as approximate coordinates. The datum was defined by loose constraints of the IGS site coordinates. This reduced the influence of possible seasonal variations of site coordinates which are not covered by linear IGS velocities.

III. VELOCITY FIELD ESTIMATION

The site velocities can be estimated only if the datum of the network has not been changed between measurement epochs. The GPS vectors must be adjusted so that the datum will remain undisturbed throughout the measurement campaigns. Usually we assume that GPS vectors define the network datum components of orientation and scale. Fluctuations in the GPS orbits could affect the orientation and scale between monitoring campaigns and therefore we assume that GPS vectors are not immune to changes in their datum content. An appropriate approach is taken to prevent the inclusion of these components in the adjustment of a 4D network. If not, the result will be an inevitable mixture between the deformation parameters and the datum components of the GPS vectors.

In this study, in each monitoring campaign the GPS vectors are incorporated into a network by utilizing only the sterilized vectors from extended free network adjustment constraints. Based on the datumless sets of coordinates, the variations in the network geometry can be modelled by means of a physical model without the influence of a datum definition inherent in geodetic measurements.

The outcome of the Bernese GPS software is a minimal constrained solution of the network points and their variance-covariance matrix for each monitoring campaign, referring to a conventional terrestrial coordinate system. By applying the extended S-Transformation to the eight monitoring campaigns, we can strip the datum content of scale and orientations from the GPS vectors and estimate a velocity field free of negative effects of those factors. The extended S-Transformation was used to transform the vector of velocities ($\dot{x}$) and its covariance matrix to a solution which is based on the network's datum definition, a datum which is based on a group of stable points. Congruency testing is performed to determine the stable datum points (for details see Even-Tzur and Reinking, 2013).

IV. DEFORMATION ANALYSIS

In two-dimensional analysis of the point velocity field we are able to compute in total six parameters of an affine transformation: the two parameters of the velocity of the network's barycenter $(\bar{\dot{x}} \quad \bar{\dot{y}})$, the rotation parameter (r_z) and the deformation rate tensor, which is composed of the scale factors of the two axes $(d^{-1}_{xx} \quad d^{-1}_{yy})$ and the angle between them (d_{xy}). The parameters gather in vector g as:

$$g=\left[\bar{\dot{x}} \quad \bar{\dot{y}} \mid r_z \mid d^{-1}_{xx} \quad d^{-1}_{yy} \mid d_{xy}\right]^T \qquad (1)$$

The scale factors present the extensions in the directions of the Cartesian coordinate axes, and the angle between them is the appropriate shearing strain.

We introduce a matrix B with the following composition:

$$B=\begin{bmatrix} 1 & 0 & -y_1 & x_1 & 0 & y_1 \\ 0 & 1 & x_1 & 0 & y_1 & x_1 \\ . & . & . & . & . & . \\ 0 & 1 & x_u & 0 & y_u & x_u \end{bmatrix} \qquad (2)$$

The coordinates x_i, and y_i of point i $(i=1,2,\ldots u)$ are given in a Cartesian system that is parallel to the reference system and with an origin at the network's barycenter.

The velocity field of a group of points can be partitioned into a linear model $B^T g$ and a residual vector v:

$$\dot{x}=Bg+v \qquad (3)$$

The velocity vector $\dot{x}$ has a cofactor matrix $Q_{\dot{x}}$ and the vector g and its cofactor matrix Q_g are given as:

$$g=(B^T Q^{-1}_{\dot{x}} B)^{-1} B^T Q^{-1}_{\dot{x}} \dot{x}$$
$$Q_g=(B^T Q^{-1}_{\dot{x}} B)^{-1}. \qquad (4)$$

For a 2D network at least three non-collinear points are required to define all the elements of vector g.

It is not obligatory to estimate all the elements of vector g for a given area represented by a velocity field of some of the network points. It might be possible that only some of the parameters better describe the motion, rotation, and deformation array in a part of the area. The structure of B allows for performing a partial solution, where only part of the six possible parameters are solved with different combinations. Different sets of parameters can be assembled and tested for suitability to the area under study.

But, how can we determine what is the best set of parameters, the one which describes best the velocity field. The problem of selecting the "best" set of parameters can be solved using the Akaike's Information Criterion (AIC) (Akaike, 1974). Since in this study we deal with a small sample size, the second-order Akaike Information Criterion (AICc) is used instead AIC (Burnham and Anderson, 2002).

AICc is defined as

$$AICc=n\cdot ln(v^T Pv)+2u(n/(n-u-1)) \qquad (5)$$

where n is the number of observations, $v^T Pv$ is the weighted sum of squared residuals and u is the number of parameters. The AICc penalizes for the addition of parameters, and thus selects a model that fits well but has a minimum number of parameters. A good mathematical model is one that has the smallest AICc score.

V. RESULTS

Eight campaigns of horizontal coordinates and their variance-covariance matrices, observed over a period of 17 years, were obtained from the GPS analysis. The data was used to derive site velocities by extended free network adjustment constraints.

The estimation of velocity field was carried out by using the Two-Steps method with an adequate estimation of the variance factor (Even-Tzur, 2004). The first step is accomplished using the Bernese GPS software. The outcome of the software is a minimal constrained solution of the network points and their variance-covariance matrix for each monitoring campaign, referring to a conventional terrestrial coordinate system. By using the extended S-transformation we can strip the datum content of scale and orientations from the measured coordinates. The solution of the network points' plane position for each monitoring epoch and their variance-covariance matrix are used as pseudo-measurements for the solution of the second step, where in each solution different models can be tested to describe the plane position of the network points.

The extraction of deformation parameters from the horizontal site velocities field was done referring to the Galilee Datum. The network points in the Carmel region were tested. In total the tested area includes 15 points (see Fig. 2).

Table 1. The surface deformation parameters that compose each set and its AICc score for the Carmel tested area.

Model (c)	**Deformation Parameters**							**AICc score**
	$\bar{x}$ [mm/yr]	$\bar{y}$ [mm/yr]	r_z 10^{-8} [rad/yr]	d^{-1}_{xx} 10^{-8} [1/yr]	d^{-1}_{yy} 10^{-8} [1/yr]	d^{-1}_{xy} 10^{-8} [1/yr]	d_{xy} 10^{-8} [rad/yr]	
1	✓	✓						149.6
2	✓	✓	✓					148.6
3	✓	✓					✓	142.9
4	✓	✓				✓		150.2
5	✓	✓	✓			✓		149.0
6	✓	✓		✓	✓			152.6
7	✓	✓	✓				✓	145.2
8	-0.63 ±0.19	0.21 ±0.16				3.7 ±0.9	4.2 ±0.6	139.2
9	✓	✓	✓	✓	✓			151.8
10	✓	✓		✓	✓		✓	142.0
11	✓	✓	✓			✓	✓	141.9
12	✓	✓	✓	✓	✓		✓	145.0

In order to define the best set of parameters, the one which describes best the velocity field, various sets of parameters were composed. The six parameters of vector g (Eq. 1) were used to create 12 sets of parameters. The deformation parameters that compose each set are presented in Table 1. The best model was determined by AICc which penalizes for the addition of parameters, and thus selects a model that fits well but has a minimum number of parameters. A good model is one that has the smallest AICc score. The AICc score of the 12 models for the Carmel tested area can be seen in Table 1 with the best set of parameters for each tested area. With a 5% level of significance, the velocity of the subnetworks' barycenter, scales and angle between the axes are significant.

VI. DISCUSSION AND CONCLUSIONS

We use principles from continuum mechanics to extract the horizontal site velocities field into surface deformation parameters. The creation of an accurate and reliable velocity field is based on eight monitoring campaigns that were measured between 1999 and 2016, eight-hour measurement sessions, measuring each network point at least twice in each campaign and using sophisticated mathematical tools. The regional site velocities were estimated with respect to a local datum that was defined by a stable cluster of sites on one side of the fault by means of extended free net adjustment constraints and extended similarity transformation.

The use of AICc allowed us to choose the best model among several. The best model is defined as the one that better describes the velocity field.

The values of velocities and deformation parameters in the research area are very small as can be seen in Table 1, yet the values are significant at a 95% confidence level.

In conclusion, the results show deformations of less than 1 mm/yr sinistral along the Carmel Fault accompanied by extensions and shear strain.

References

Akaike, H., 1974. A new look at the statistical model identification. IEEE transactions on automatic control, 19 (6), 716–723.

Burnham, K.P. and Anderson, D.R., 2002. Model Selection and Multimodel Inference: A Practical-Theoretic Approach, 2nd Ed. Springer, New York, 496 p.

Dach, R., Lutz, S., Walser, P., Fridez, P., 2007. Bernese GNSS Software Version 5.2. Astronomical Institute, University Bern, http://www.bernese.unibe.ch/docs/DOCU52.pdf.

Even-Tzur, G., 2004. Variance Factor Estimation for Two-Step Analysis of Deformation Networks. Journal of surveying engineering. Journal of Surveying Engineering, 130(3):113-118.

Even-Tzur, G., 2011. Deformation Analysis by Means of Extended Free Network Adjustment Constraints, Journal of Surveying Engineering 137, 47–52.

Even-Tzur, G., 2012. Extended S-Transformation as a Tool for Deformation Analysis, Survey review 44, 315–318.

Even-Tzur, G. and Reinking, J., 2013. Velocity field across the Carmel fault calculated by extended free network adjustment constraints. Journal of Applied Geodesy, 7(2), pp.75-82.

Fleischer, L. and Gafsou, R., 2005. Structural map on top Judea Group. In: Hall, J.K., Krasheninnikov, V.A., Hirsch, F., Benjamini, Ch., Flexer, A. (eds.), Geological Framework of the Levant, Plates (Plate V). Historical Productions-Hall, Jerusalem.

Hofstetter, A., van Eck, T., Shapira, A., 1996. Seismic activity along the fault branches of the Dead Sea –Jordan transform: the Carmel–Tirtza fault system. Tectonophysics, 267, 317–330.

Rotstein, Y., Shaliv, G., Rybakov, M., 2004. Active tectonics of the Yizre'el valley, Israel, using high-resolution seismic reflection data. Tectonophysics 382, 31–50.

Segev, A., Lyakhovsky, V. and Weinberger, R., 2014. Continental transform–rift interaction adjacent to a continental margin: The Levant case study. Earth-Science Reviews, 139, pp.83-103.

Segev, A. and Rybakov, M., 2011. History of faulting and magmatism in the Galilee (Israel) and across the Levant continental margin inferred from potential field data. Journal of Geodynamics, 51(4), pp.264-284.

Segev, A., Rybakov, M., Lyakhovsky, V., Hofstetter, A., Tibor, G., Goldshmidt, V., Ben- Avraham, Z., 2006. The structure, isostasy and gravity field of the Levant continental margin and the southeast Mediterranean area. Tectonophysics 425, 137–157.

Wolf, H., 1977. Eindeutige und mehrdeutige Geodätische Netze. Adh. Braunschw. Wiss. Ges., Band 28.